Acta Crystallographica Section B
Structural Science
ISSN 0108-7681

Oligosiloxanediols as building blocks for supramolecular chemistry: hydrogen-bonded adducts with amines form supramolecular structures in zero, one and two dimensions

Brian O'Leary,[a] Trevor R. Spalding,[a] George Ferguson[b]† and Christopher Glidewell[b]*

[a]Chemistry Department, University College, Cork, Ireland, and [b]School of Chemistry, University of St Andrews, St Andrews, Fife KY16 9ST, Scotland

† On leave from: Department of Chemistry and Biochemistry, University of Guelph, Guelph, Ontario, Canada N1G 2W1.

Correspondence e-mail: cg@st-andrews.ac.uk

Received 5 July 1999
Accepted 13 October 1999

The structure of 1,1,3,3,5,5-hexaphenyltrisiloxane-1,5-diol–pyrazine (4/1), $(C_{36}H_{32}O_4Si_3)_4\cdot C_4H_4N_2$ (1), contains finite centrosymmetric aggregates; the diol units form dimers, by means of O—H···O hydrogen bonds, and pairs of such dimers are linked to the pyrazine by means of O—H···N hydrogen bonds. In 1,1,3,3,5,5-hexaphenyltrisiloxane-1,5-diol–pyridine (2/3), $(C_{36}H_{32}O_4Si_3)_2\cdot(C_5H_5N)_3$ (2), the diol units are linked into centrosymmetric pairs by means of disordered O—H···O hydrogen bonds: two of the three pyridine molecules are linked to the diol dimer by means of ordered O—H···N hydrogen bonds, while the third pyridine unit, which is disordered across a centre of inversion, links the diol dimers into a $C_3^3(9)$ chain by means of O—H···N and C—H···O hydrogen bonds. In 1,1,3,3-tetraphenyldisiloxane-1,3-diol–hexamethylenetetramine (1/1), $(C_{24}H_{22}O_3Si_2)\cdot C_6H_{12}N_4$ (3), the diol acts as a double donor and the hexamethylenetetramine acts as a double acceptor in ordered O—H···N hydrogen bonds and the structure consists of $C_2^2(10)$ chains of alternating diol and amine units. In 1,1,3,3-tetraphenyldisiloxane-1,3-diol–2,2′-bipyridyl (1/1), $C_{24}H_{22}O_3Si_2\cdot C_{10}H_8N_2$ (4), there are two independent diol molecules, both lying across centres of inversion and therefore both containing linear Si—O—Si groups: each diol acts as a double donor of hydrogen bonds and the unique 2,2′-bipyridyl molecule acts as a double acceptor, thus forming $C_2^2(11)$ chains of alternating diol and amine units. The structural motif in 1,1,3,3-tetraphenyldisiloxane-1,3-diol–pyrazine (2/1), $(C_{24}H_{22}O_3Si_2)_2\cdot C_4H_4N_2$ (5), is a chain-of-rings: pairs of diol molecules are linked by O—H···O hydrogen bonds into centrosymmetric $R_2^2(12)$ dimers and these dimers are linked into $C_2^2(13)$ chains by means of O—H···N hydrogen bonds to the pyrazine units. 1,1,3,3-Tetraphenyldisiloxane-1,3-diol–pyridine (1/1), $C_{24}H_{22}O_3Si_2\cdot C_5H_5N$ (6), and 1,1,3,3-tetraphenyldisiloxane-1,3-diol–pyrimidine (1/1), $C_{24}H_{22}O_3Si_2\cdot C_4H_4N_2$ (7), are isomorphous: in each compound the amine unit is disordered across a centre of inversion. The diol molecules form $C(6)$ chains, by means of disordered O—H···O hydrogen bonds, and these chains are linked into two-dimensional nets built from $R_6^6(26)$ rings, by a combination of O—H···N and C—H···O hydrogen bonds.

1. Introduction

The structures of tetraorganodisiloxane-1,3-diols, HOSiR_2-OSiR_2OH, exhibit a wide range of hydrogen-bonding patterns (Lickiss, 1995). The commonest pattern of molecular aggregation, exhibited for example by both $HOSiMe_2OSiMe_2OH$ (Lickiss *et al.*, 1993) and $HOSiPh_2OSiPh_2OH$ (Hossain & Hursthouse, 1988), consists of double chains of molecules in which each hydroxyl group acts as both a hydrogen-bond

Table 1
Experimental details.

	(1)	(2)	(3)	(4)
Crystal data				
Chemical formula	$4(C_{36}H_{32}O_4Si_3)\cdot C_4H_4N_2$	$2(C_{36}H_{32}O_4Si_3)\cdot 3(C_5H_5N)$	$C_{24}H_{22}O_3Si_2\cdot C_6H_{12}N_4$	$C_{24}H_{22}O_3Si_2\cdot C_{10}H_8N_2$
Chemical formula weight	2531.64	1463.07	554.79	570.78
Cell setting	Triclinic	Triclinic	Monoclinic	Triclinic
Space group	$P\overline{1}$	$P\overline{1}$	$P2_1/c$	$P\overline{1}$
a (Å)	14.2354 (10)	10.7764 (10)	16.1555 (9)	8.9245 (8)
b (Å)	15.2960 (14)	12.8122 (12)	8.4622 (10)	10.1900 (17)
c (Å)	18.7470 (14)	15.1733 (13)	21.8427 (16)	17.3660 (19)
α (°)	71.764 (6)	91.999 (11)	90	99.57 (2)
β (°)	88.862 (6)	94.851 (13)	97.386 (5)	100.519 (13)
γ (°)	62.544 (7)	109.063 (7)	90	93.80 (3)
V (Å^3)	3402.7 (5)	1968.6 (3)	2961.4 (4)	1523.5 (3)
Z	1	1	4	2
D_x (Mg m^{-3})	1.235	1.234	1.244	1.244
Radiation type	Mo $K\alpha$	Mo $K\alpha$	Mo $K\alpha$	Mo $K\alpha$
Wavelength (Å)	0.71073	0.71073	0.71073	0.71073
No. of reflections for cell parameters	25	25	25	25
θ range (°)	9.30–19.80	9.65–16.70	9.35–14.20	9.30–19.25
μ (mm^{-1})	0.178	0.164	0.157	0.153
Temperature (K)	294 (1)	294 (1)	294 (1)	294 (1)
Crystal form	Block	Block	Block	Block
Crystal size (mm)	0.36 × 0.33 × 0.29	0.36 × 0.34 × 0.30	0.34 × 0.32 × 0.20	0.38 × 0.36 × 0.33
Crystal colour	Colourless	Colourless	Colourless	Colourless
Data collection				
Diffractometer	Enraf–Nonius CAD-4	Enraf–Nonius CAD-4	Enraf–Nonius CAD-4	Enraf–Nonius CAD-4
Data collection method	$\theta/2\theta$ scans	$\theta/2\theta$ scans	$\theta/2\theta$ scans	$\theta/2\theta$ scans
Absorption correction	None	None	None	None
No. of measured reflections	14788	8519	6651	6633
No. of independent reflections	14788	8519	6436	6633
No. of observed reflections	10215	5535	3416	5141
Criterion for observed reflections	$I > 2\sigma(I)$	$I > 2\sigma(I)$	$I > 2\sigma(I)$	$I > 2\sigma(I)$
R_{int}	0.000	0.000	0.012	0.000
θ_{max} (°)	26.92	26.89	26.90	26.93
Range of h, k, l	$-16 \rightarrow h \rightarrow 18$ $0 \rightarrow k \rightarrow 19$ $-22 \rightarrow l \rightarrow 23$	$-13 \rightarrow h \rightarrow 12$ $0 \rightarrow k \rightarrow 16$ $-19 \rightarrow l \rightarrow 19$	$-20 \rightarrow h \rightarrow 20$ $0 \rightarrow k \rightarrow 10$ $0 \rightarrow l \rightarrow 27$	$-11 \rightarrow h \rightarrow 11$ $0 \rightarrow k \rightarrow 13$ $-22 \rightarrow l \rightarrow 21$
No. of standard reflections	3	3	3	3
Frequency of standard reflections	Every 120 min	Every 120 min	Every 120 min	Every 120 min
Intensity decay (%)	0	3	6.9	2.8
Refinement				
Refinement on	F^2	F^2	F^2	F^2
$R[F^2>2\sigma(F^2)]$	0.0401	0.0434	0.0443	0.0365
$wR(F^2)$	0.1203	0.1178	0.1156	0.1166
S	1.077	1.055	0.946	1.104
No. of reflections used in refinement	14788	8519	6436	6633
No. of parameters used	807	472	409	376
H-atom treatment	H atoms constrained	H atoms constrained	H atoms constrained	H atoms constrained
Weighting scheme	$w = 1/[\sigma^2(F_o^2) + (0.0698P)^2 + 0.0963P]$, where $P=(F_o^2+2F_c^2)/3$	$w = 1/[\sigma^2(F_o^2) + (0.0588P)^2 + 0.1381P]$, where $P=(F_o^2+2F_c^2)/3$	$w = 1/[\sigma^2(F_o^2) + (0.0585P)^2]$, where $P = (F_o^2 + 2F_c^2)/3$	$w = 1/[\sigma^2(F_o^2) + (0.0593P)^2 + 0.2883P]$, where $P=(F_o^2+2F_c^2)/3$
$(\Delta/\sigma)_{max}$	0.003	0.000	0.048	0.001
$\Delta\rho_{max}$ (e Å^{-3})	0.263	0.343	0.259	0.279
$\Delta\rho_{min}$ (e Å^{-3})	−0.264	−0.286	−0.238	−0.213
Extinction method	*SHELXL*97 (Sheldrick, 1997)	*SHELXL*97 (Sheldrick, 1997)	*SHELXL*97 (Sheldrick, 1997)	*SHELXL*97 (Sheldrick, 1997)
Extinction coefficient	0.0225 (9)	0.0040 (7)	0.0027 (6)	0.0078 (14)
Source of atomic scattering factors	*International Tables for Crystallography* (1992, Vol. C, Tables 4.2.6.8 and 6.1.1.4)	*International Tables for Crystallography* (1992, Vol. C, Tables 4.2.6.8 and 6.1.1.4)	*International Tables for Crystallography* (1992, Vol. C, Tables 4.2.6.8 and 6.1.1.4)	*International Tables for Crystallography* (1992, Vol. C, Tables 4.2.6.8 and 6.1.1.4)

Table 1 (continued)

	(5)	(6)	(7)
Crystal data			
Chemical formula	$2(C_{24}H_{22}O_3Si_2)\cdot C_4H_4N_2$	$C_{24}H_{22}O_3Si_2\cdot C_5H_5N$	$C_{24}H_{22}O_3Si_2\cdot C_4H_4N_2$
Chemical formula weight	909.28	493.70	494.69
Cell setting	Triclinic	Triclinic	Triclinic
Space group	$P\overline{1}$	$P\overline{1}$	$P\overline{1}$
a (Å)	8.8365 (8)	6.4469 (15)	6.4358 (5)
b (Å)	10.8028 (10)	10.2837 (15)	10.2497 (12)
c (Å)	13.3231 (16)	10.6088 (15)	10.4056 (10)
α (°)	108.740 (11)	74.645 (11)	76.000 (7)
β (°)	89.774 (14)	81.968 (13)	84.438 (9)
γ (°)	94.792 (10)	85.511 (11)	86.372 (12)
V (Å^3)	1199.8 (2)	671.0 (2)	662.32 (11)
Z	1	1	1
D_x (Mg m^{-3})	1.258	1.222	1.240
Radiation type	Mo $K\alpha$	Mo $K\alpha$	Mo $K\alpha$
Wavelength (Å)	0.71073	0.71073	0.71073
No. of reflections for cell parameters	25	25	25
θ range (°)	14.50–20.50	10.0–19.0	9.50–17.0
μ (mm^{-1})	0.175	0.162	0.165
Temperature (K)	294 (1)	294 (1)	294 (1)
Crystal form	Plate	Block	Block
Crystal size (mm)	0.39 × 0.39 × 0.10	0.35 × 0.35 × 0.33	0.38 × 0.38 × 0.36
Crystal colour	Colourless	Colourless	Colourless
Data collection			
Diffractometer	Enraf–Nonius CAD-4	Enraf–Nonius CAD-4	Enraf–Nonius CAD-4
Data collection method	$\theta/2\theta$ scans	$\theta/2\theta$ scans	$\theta/2\theta$ scans
Absorption correction	None	None	None
No. of measured reflections	5200	2899	2876
No. of independent reflections	5200	2899	2876
No. of observed reflections	3278	2449	2389
Criterion for observed reflections	$I > 2\sigma(I)$	$I > 2\sigma(I)$	$I > 2\sigma(I)$
R_{int}	0.000	0.000	0.000
θ_{max} (°)	26.89	26.88	26.91
Range of h, k, l	$-11 \rightarrow h \rightarrow 11$ $0 \rightarrow k \rightarrow 13$ $-16 \rightarrow l \rightarrow 16$	$-8 \rightarrow h \rightarrow 8$ $0 \rightarrow k \rightarrow 13$ $-12 \rightarrow l \rightarrow 13$	$-8 \rightarrow h \rightarrow 8$ $0 \rightarrow k \rightarrow 13$ $-12 \rightarrow l \rightarrow 13$
No. of standard reflections	3	3	3
Frequency of standard reflections	Every 120 min	Every 120 min	Every 60 min
Intensity decay (%)	0	0	0
Refinement			
Refinement on	F^2	F^2	F^2
$R[F^2 > 2\sigma(F^2)]$	0.0411	0.0403	0.0423
$wR(F^2)$	0.1117	0.1094	0.1311
S	1.038	1.069	1.051
No. of reflections used in refinement	5200	2899	2876
No. of parameters used	292	163	162
H-atom treatment	H atoms constrained	H atoms constrained	H atoms constrained
Weighting scheme	$w = 1/[\sigma^2(F_o^2) + (0.0577P)^2]$, where $P = (F_o^2 + 2F_c^2)/3$	$w = 1/[\sigma^2(F_o^2) + (0.0522P)^2 + 0.1916P]$, where $P = (F_o^2 + 2F_c^2)/3$	$w = 1/[\sigma^2(F_o^2) + (0.0802P)^2 + 0.1328P]$, where $P = (F_o^2 + 2F_c^2)/3$
$(\Delta/\sigma)_{max}$	0.000	0.000	0.001
$\Delta\rho_{max}$ (e Å^{-3})	0.250	0.295	0.319
$\Delta\rho_{min}$ (e Å^{-3})	−0.210	−0.258	−0.388
Extinction method	*SHELXL*97 (Sheldrick, 1997)	*SHELXL*97 (Sheldrick, 1997)	*SHELXL*97 (Sheldrick, 1997)
Extinction coefficient	0.010 (2)	0.034 (5)	0.028 (6)
Source of atomic scattering factors	*International Tables for Crystallography* (1992, Vol. C, Tables 4.2.6.8 and 6.1.1.4)	*International Tables for Crystallography* (1992, Vol. C, Tables 4.2.6.8 and 6.1.1.4)	*International Tables for Crystallography* (1992, Vol. C, Tables 4.2.6.8 and 6.1.1.4)

donor and a hydrogen-bond acceptor. In $HOSiMe_2OSiMe_2OH$ the double chain is generated by the action of a 2_1 screw axis and the hydrogen-bonding motif is of $C_2^2(4)$ type (Bernstein *et al.*, 1995). In $HOSiPh_2OSiPh_2OH$, where there are three independent molecules in the asymmetric unit, there appears to be a similar pattern of hydrogen bonds, although the hydroxyl H atoms were not unambiguously located (Hossain & Hursthouse, 1988); the numerous close O···O

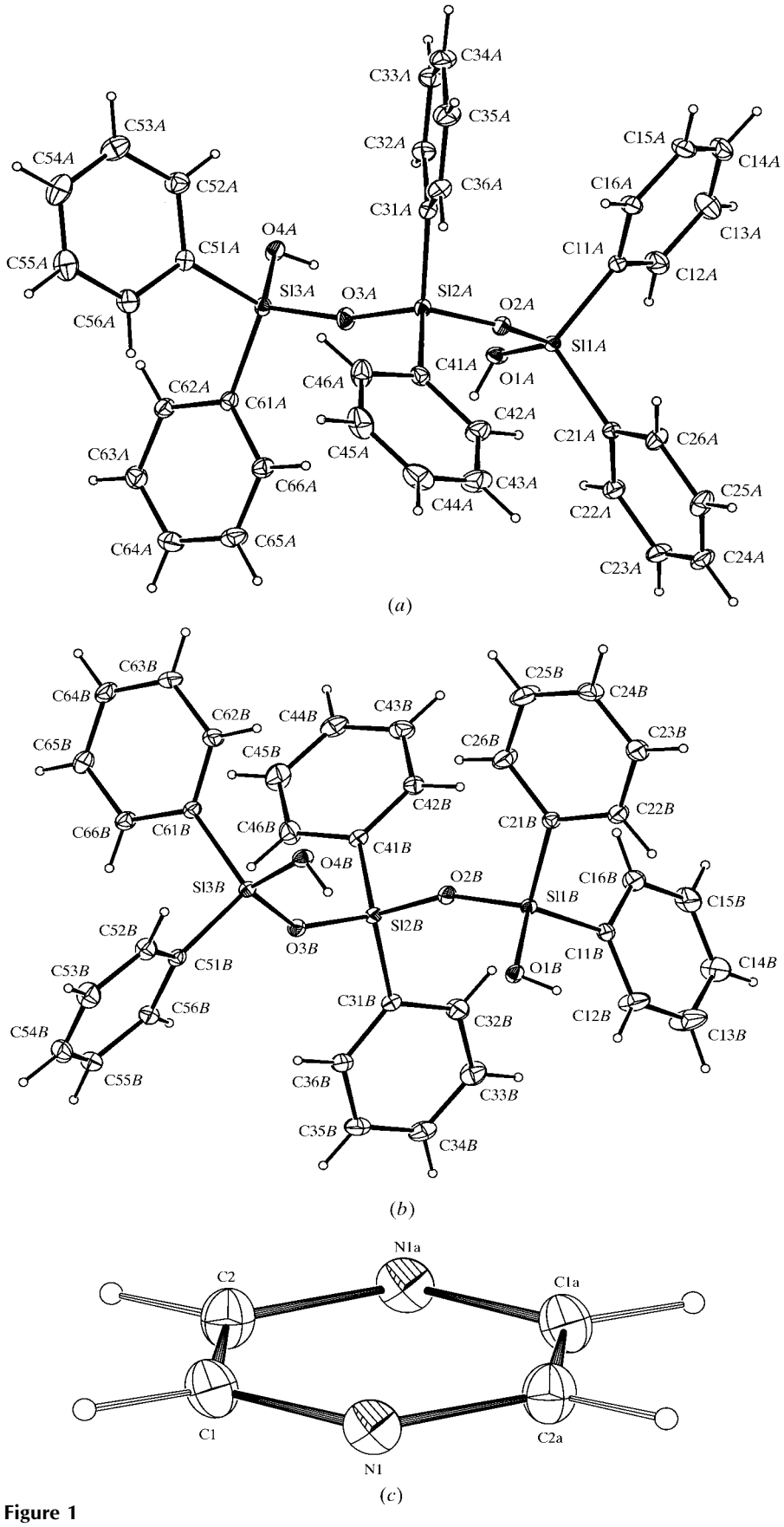

Figure 1
The molecular components of (1), showing the atom-labelling scheme: (*a*) siloxanediol A, (*b*) siloxanediol B and (*c*) pyrazine. Displacement ellipsoids are drawn at the 30% probability level.

contacts across inversion centres indicate that at least some of the hydroxyl H atoms are disordered.

By contrast to these long-chain structures, the related hexaphenyltrisiloxane-1,5-diol $HOSiPh_2OSiPh_2OSiPh_2OH$ (Behbehani *et al.*, 1993) consists of dimers: each molecule contains an intramolecular O—H···O hydrogen bond and these molecules are linked by intermolecular O—H···O hydrogen bonds into centrosymmetric dimers. The hydrogen-bonding pattern within the dimer unit can be assigned the graph-set descriptors $N_1 = S(8)D$, $N_2 = R_4^4(8)$ (Bernstein *et al.*, 1995), so that this dimer is, in fact, isographic with the dimer of the ferrocenediol $Fe(C_5H_4CPh_2OH)_2$ (Ferguson *et al.*, 1993*a*).

This ferrocenediol readily forms hydrogen-bonded adducts with a wide range of nitrogenous bases (Ferguson *et al.*, 1993*b*; Glidewell *et al.*, 1994; Ferguson *et al.*, 1995): since, in general, silanols are somewhat more acidic than the corresponding carbinols, it may be expected that both $HOSiPh_2OSiPh_2OH$ and $HOSiPh_2OSiPh_2OSiPh_2OH$ will form hydrogen-bonded adducts with nitrogenous bases even more readily than $Fe(C_5H_4CPh_2OH)_2$. The structure of one such adduct, a 3:2 complex of $HOSiPh_2OSiPh_2OH$ with pyridazine, has in fact been reported (Ruud *et al.*, 1991): however, the poor quality of the X-ray data [R = 0.060 with a data-to-parameter ratio (n/p) of only 3.05; σ(Si—C) 0.01–0.02 Å] meant that no H-atom sites could be identified, although the hydrogen-bond locations were readily inferred from the non-bonded distances.

In this paper we report the synthesis and structural characterization of hydrogen-bonded adducts formed by the oligosiloxanediols $HO(SiPh_2O)_nH$ (n = 2 and 3) with a range of ring and cage amines. 1,1,3,3,5,5-Hexaphenyltrisiloxane-1,5-diol–pyrazine (4/1) (1) forms a finite, zero-dimensional aggregate; one-dimensional aggregates in the form of chains are formed by 1,1,3,3,5,5-hexaphenyltrisiloxane-1,5-diol–pyridine (2/3) (2), 1,1,3,3-tetraphenyldisiloxane-1,3-diol–hexamethylenetetramine (1/1) (3) and 1,1,3,3-tetraphenyldisiloxane-1,3-diol–2,2′-bipyridyl (1/1) (4); a

Table 2
Hydrogen-bond parameters (Å, °).

Compound (1)					
O1*A*···N1	2.706 (2)	H1*A*···N1	1.96	O1*A*—H1*A*···N1	150
O1*B*···O1*A*	2.673 (2)	H1*B*···O1*A*	1.95	O1*B*—H1*B*···O1*A*	146
O4*A*···O1*B*	2.700 (2)	H4*A*···O1*B*	1.92	O4*A*—H4*A*···O1*B*	157
O4*B*···O4*A*	2.794 (2)	H4*B*···O4*A*	1.88	O4*B*—H4*B*···O4*A*	174
Compound (2)					
O4···N71	2.722 (3)	H4···N71	1.98	O4—H4···N71	150
O1···O1^{i}	2.809 (2)	H1···O1^{i}	2.01	O1—H1···O1^{i}	164
O1···N81	3.048 (4)	H2···N81	2.23	O1—H2···N81	173
C81···O1	3.048 (4)	H81···O1	2.13	C81—H81···O1	167
Compound (3)					
O1···N1	2.804 (2)	H1···N1	2.10	O1—H1···N1	144
O2···N2^{ii}	2.731 (2)	H2···N2^{ii}	1.96	O2—H2···N2^{ii}	156
Compound (4)					
O1···N51	2.869 (2)	H1···N51	2.08	O1—H1···N51	159
O2···N61	2.846 (2)	H2···N61	2.04	O2—H2···N61	167
Compound (5)					
O1···N51	2.720 (2)	H1···N51	1.94	O1—H1···N51	159
O2···O1^{iii}	2.800 (2)	H2···O1^{iii}	1.99	O2—H2···O1^{iii}	167
Compound (6)					
O2···O2^{iv}	2.755 (2)	H1···O2^{iv}	1.94	O2—H1···O2^{iv}	170
O2···N31	2.995 (3)	H2···N31	2.18	O2—H2···N31	172
C31···O2	2.995 (3)	H31···O2	2.14	C31—H31···O2	174
Compound (7)					
O2···O2^{iv}	2.736 (2)	H1···O2^{iv}	1.92	O2—H1···O2^{iv}	170
O2···N31	2.959 (4)	H2···N31	2.17	O2—H2···N31	163
C31···O2	2.959 (4)	H31···O2	2.10	C31—H31···O2	174

Symmetry codes: (i) $-x, -y, -z$; (ii) $x, -1+y, z$; (iii) $-x, -y, 1-z$; (iv) $-x, 1-y, 1-z$.

one-dimensional chain-of-rings is formed by 1,1,3,3-tetraphenyldisiloxane-1,3-diol–pyrazine (2/1) (5); and continuous two-dimensional sheet structures are formed by the isomorphous 1,1,3,3-tetraphenyldisiloxane-1,3-diol–pyridine (1/1) (6) and 1,1,3,3-tetraphenyldisiloxane-1,3-diol–pyrimidine (1/1) (7).

2. Experimental

2.1. Syntheses

2.1.1. Diols. 1,1,3,3-Tetraphenyldisiloxane-1,3-diol was prepared by hydrolysis of 1,3-dichloro-1,1,3,3,-tetraphenyldisiloxane using a stoichiometric quantity of water in acetone, followed by crystallization from CH_2Cl_2/hexane (1/2 v/v): m.p. 385–387 K (lit.: 388 K; Harris, 1963). 1,1,3,3,5,5-Hexaphenyltrisiloxane-1,5-diol was prepared according to the published procedure (Selin, 1977): after crystallization from ether/cyclohexane: (1/3 v/v) m.p. 384–386 K (lit.: 385–386 K; Selin, 1977).

2.1.2. Adducts. Compound (1): Stoichiometric quantities of the trisiloxanediol and pyrazine were dissolved in ether, and after 3 h the solution was concentrated to a viscous oil. Extraction into CH_2Cl_2/heptane (1/1 v/v) followed by crystallization yielded (1), m.p. 376–378 K. Analysis: found C 70.4, H 5.2, N 1.0%; $C_{148}H_{132}N_2O_{16}Si_{12}$ requires C 70.2, H 5.3, N 1.1%.

Compound (2): Stoichiometric quantities of the trisiloxanediol and pyridine were dissolved in ether, and after 4 h the solution was concentrated until a white solid just began to form: extraction into CH_2Cl_2/heptane (1/1 v/v) followed by crystallization gave (2), m.p. 361–364 K. Analysis: found C 71.6, H 5.5, N 2.9%; $C_{87}H_{79}N_3O_8Si_6$ requires C 71.6, H 5.3, N 2.9%.

Compound (3): Equimolar quantities of the disiloxanediol and hexamethylenetetramine were dissolved in CH_2Cl_2, and after 10 h the solution was concentrated to a viscous oil. Extraction into CH_2Cl_2/toluene/cyclohexane (1/1/3 v/v) followed by crystallization gave firstly unreacted HMTA and then (3), m.p. 354–356 K. Analysis: found C 64.7, H 6.3, N 10.3%; $C_{30}H_{34}N_4O_3Si_2$ requires C 64.9, H 6.2, N 10.1%.

Compound (4): Equimolar quantities of the disiloxanediol and of 2,2′-bipyridyl were dissolved in ether, and after 6 h the solution was concentrated to a viscous oil. Addition of ice-cold hexane yielded a white powder and recrystallization of this from toluene/hexane (1/3 v/v) gave (4), m.p. 343–345 K. Analysis: found C 71.2, H 5.4, N 4.9%; $C_{34}H_{30}N_2O_3Si_2$ requires C 71.5, H 5.3, N 4.9%.

Compound (5): Stoichiometric quantities of the disiloxanediol and of pyrazine were dissolved in ether, and after 5 h the solution was concentrated to give a sticky white solid. Crystallization from toluene/hexane (1/2 v/v) yielded (5), m.p. 373–375 K. Analysis: found C 68.5, H 5.4, N 3.1%; $C_{52}H_{48}N_2O_6Si_4$ requires C 68.7, H 5.3, N 3.1%.

Compound (6): A stoichiometric quantity of pyridine was added to a solution of the disiloxanediol in ether, and after 5 h

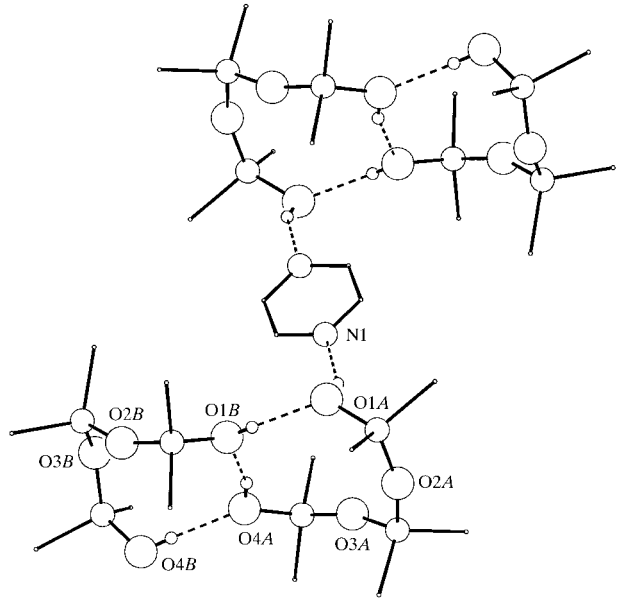

Figure 2
The finite molecular aggregate in (1). For the sake of clarity, only the C*n*1*A* and C*n*1*B* (*n* = 1–6) atoms of the phenyl rings are shown; the H atoms of the pyrazine component are also omitted.

the solution was concentrated to a viscous oil. This oil was dissolved in toluene, and layering with hexane yielded crystals of (6), m.p. 396–398 K (lit.: 396–398 K; Prescott & Selin, 1965). Analysis: found C 70.8, H 5.7, N 3.0%; $C_{29}H_{27}NO_3Si_2$ requires C 70.5, H 5.5, N 2.8%.

Compound (7): Equimolar quantities of the disiloxanediol and pyrimidine were dissolved in ether, and after 5 h the solution was concentrated to a viscous residue. Extraction into toluene/hexane (1/2 v/v) followed by crystallization gave (7), m.p. 353–355 K. Analysis: found C 68.1, H 5.3, N 5.7%; $C_{28}H_{26}N_2O_3Si_2$ requires C 68.0, H 5.3, N 5.7%.

2.2. Data collection, structure solution and refinement

Details of data collection, and structure solution and refinement are summarized in Table 1.[1] For (3) the space group $P2_1/c$ was uniquely determined from the systematic absences. Compounds (1), (2) and (4)–(7) are all triclinic: for each the space group $P\bar{1}$ was chosen and confirmed by the successful structure solution and refinement.

In (2), one of the pyridine units (that containing N81) lies across a centre of inversion and is therefore disordered: similarly in (6) the unique pyridine lies across a centre of inversion, while in (7) the pyrimidine not only lies across a centre of inversion, but also exhibits rotational disorder. For each of (2), (6) and (7) difference maps showed clearly that the atom sites in the alternative orientations of the pyridine in (2) and (6), and in the four orientations of the pyrimidine in (7), were essentially coincident: in other words the centres of inversion in each case lies at the centroid of the heteroaromatic ring. Therefore, the disordered pyridine molecule in both (2) and (6) was modelled by a ring in which sites 1 and 4 were each occupied by (0.5 C + 0.5 N); similarly, the pyrimidine in (7) was modelled by a ring in which sites 1 and 4 were occupied by (0.5 C + 0.5 N), and sites 2, 3, 5 and 6 were occupied by (0.75 C + 0.25 N). In each of the mixed-occupancy sites in (2), (6) and (7), the alternative occupants, C or N, were constrained to have identical atom coordinates and in addition the two occupants of each site were constrained to have identical anisotropic displacement parameters: in effect each such site was occupied by a single atom having a composite atomic scattering factor.

In (3) one of the phenyl rings (that containing C21–C26) was found to exhibit orientational disorder, occupying two sets of sites with equal occupancy, although there was no trace of any disorder in the other phenyl rings in this compound. This disorder was modelled by means of two independent rings C2*nA* and C2*nB* (for n = 1–6), freely refined except that Si1 was restrained to lie in the plane of each ring, C2*nA* and C2*nB*.

For each of (1)–(7), careful inspection of difference maps in the vicinity of the nitrogen and the hydroxylic O atoms showed (*a*) that there was no evidence whatever for any transfer of H atoms from O to N, (*b*) that in (2) the hydroxyl H atom bonded to O1 was disordered over two sites, labelled H1 and H2, with equal occupancy, and (*c*) that in each of (6) and (7) the unique hydroxyl H atoms were similarly disordered, in each case over two equally populated sites.

In the final refinement cycles, H atoms were treated as riding atoms (C—H 0.93 and 0.97, N—H 0.89 and 0.90, O—H 0.82 Å). Table 2 contains details of the hydrogen bonding and Table 3 presents selected molecular dimensions. Figs. 1, 3, 5, 7, 11 and 12 show the asymmetric units of (1)–(7), and Figs. 2, 4, 6, 8, 10 and 13 show aspects of the crystal structures.

3. Results and discussion

3.1. Supramolecular structures

It is convenient to consider the adducts in terms of the dimensionality of the supramolecular aggregates. Since the trisiloxanediol is able, because of its molecular chain length, to form intramolecular O—H···O hydrogen bonds, this opens the possibility that the supramolecular aggregates formed by this diol can be finite and zero-dimensional, in the sense that there is no necessity to form extended structures (chains, sheets or frameworks). The aggregates formed by the disiloxanediol, on the other hand, are all likely to be at least one-dimensional, as the diol is unable to form intramolecular hydrogen bonds. To this extent, the general pattern of behaviour of these two diols reflects the differences observed in the structures of the pure substances (Hossain & Hursthouse, 1988; Behbehani *et al.*, 1993).

3.1.1. 1,1,3,3,5,5-Hexaphenyltrisiloxane-1,5-diol–pyrazine (4/1) (1). The centrosymmetric aggregate in (1) contains four molecules of the diol and one molecule of

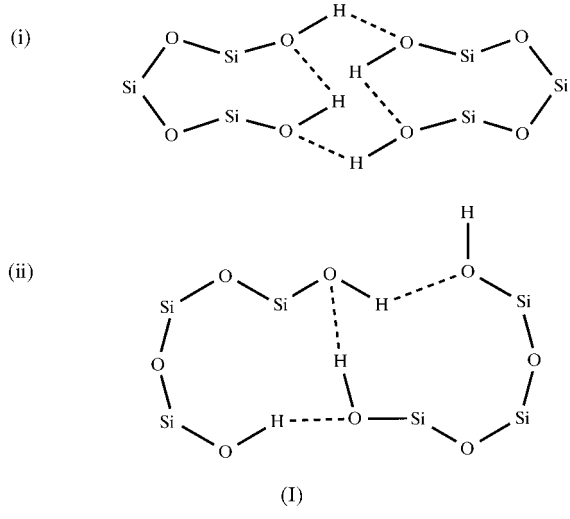

(I)

pyrazine (Fig. 1): the asymmetric unit thus consists of two diol molecules and one half of a pyrazine molecule. The aggregate is conveniently regarded as a pair of hydrogen-bonded diol dimers linked by the pyrazine (Fig. 2). However, the construction of the diol–dimer unit in (1) is significantly different from that of the centrosymmetric dimer found in the pure diol [Behbehani *et al.*, 1993; Scheme I(i)]. In the pure

[1] Supplementary data for this paper are available from the IUCr electronic archives (Reference: CF0008). Services for accessing these data are described at the back of the journal.

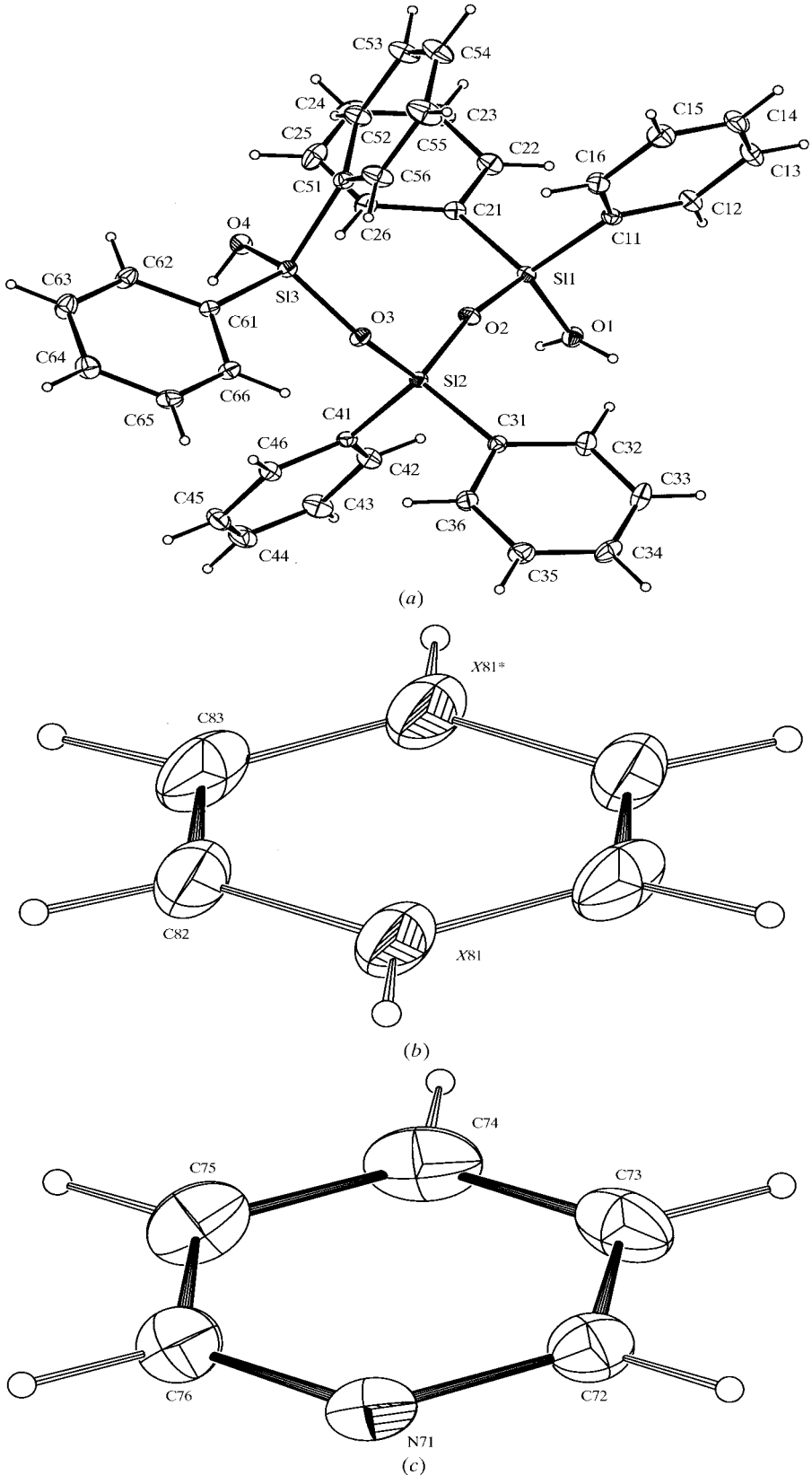

Figure 3
The molecular components of (2), showing the atom-labelling scheme: (*a*) the siloxanediol, (*b*) the disordered pyridine and (*c*) the ordered pyridine. The site labelled *X*81 is occupied by ($\frac{1}{2}$C + $\frac{1}{2}$N) and the associated site H81 has $\frac{1}{2}$ occupancy. Only one orientation of the disordered pyridine is shown. Atoms are depicted as in Fig. 1: the site labelled with a star (*) is at symmetry position $(-1-x, -y, -z)$.

diol, each molecule forms an intramolecular O—H···O hydrogen bonds in an *S*(8) motif (Bernstein *et al.*, 1995), and two such molecules are then linked by paired intermolecular hydrogen bonds in an $R_4^4(8)$ motif, so that each hydroxylic O atom acts as both donor and acceptor of O—H···O hydrogen bonds. In (1), by contrast, there are no intramolecular O—H···O hydrogen bonds at all: instead molecule *B* (Figs. 1 and 2) acts as a double donor towards molecule *A*, while molecule *A* acts a single donor to molecule *B*, in an O—H···O hydrogen bond, and as a single donor to pyrazine in an O—H···N hydrogen bond. There is thus an $R_2^2(16)$ ring divided into two $R_2^2(10)$ sectors and having a single hydrogen bond, O4*A*···O1*B*, in common [Scheme I(ii)]. Atom O4*B* acts only as a donor of hydrogen bonds, but the other three hydroxylic O atoms act as both donors and acceptors, while N1 acts as the fourth acceptor. The three O—H···O and one O—H···N hydrogen bonds thus utilize all the donor capacity, and hence there are no hydrogen-bonding interactions between these centrosymmetric five-component aggregates.

3.1.2. 1,1,3,3,5,5-Hexaphenyltrisiloxane-1,5-diol–pyridine (2/3) (2). The asymmetric unit in (2) (Fig. 3) consists of one molecule each of pyridine and the diol, both lying in general positions, together with one half of a pyridine molecule disordered across a centre of inversion in space group $P\bar{1}$, such that the ring centroid is coincident with the inversion centre. The two components in general positions are linked by an O–H···N hydrogen bond: O4 acts as hydrogen-bond donor to N71, and H4 is fully ordered: however, the linking of the diol units to the third pyridine molecule gives rise to some complexity.

In analysing the supramolecular structure (Fig. 4) it is convenient to consider first the interactions linking into four-molecule aggregates the molecular components which lie in general positions, and then to consider the effect of the centrosymmetric and disordered pyridine units in connecting together the four-molecule aggregates. The ordered pyridine and the diol are linked by an O—H···N hydrogen bond, and a pair of

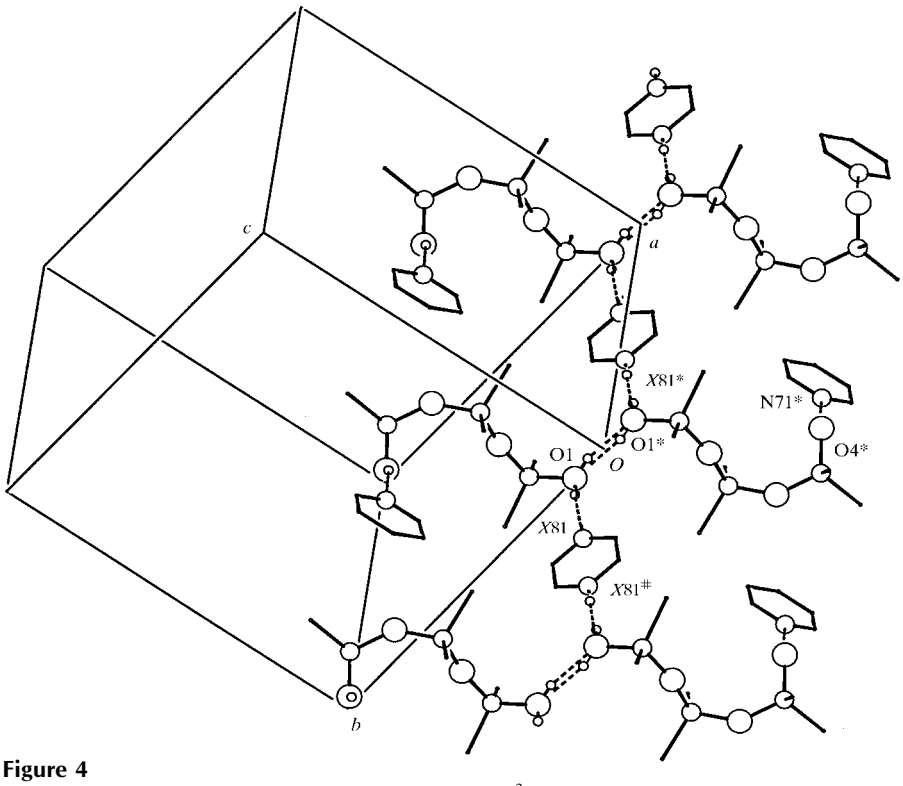

Figure 4
Part of the crystal structure of (2), showing one of the $C_3^3(9)$ chains parallel to [100]. For the sake of clarity, only the C*n*1 (n = 1–6) atoms of the phenyl rings are shown; the ordered H atoms of the pyridine components are also omitted. The sites labelled with a star (*) or hash (#) are at symmetry positions $(-x, -y, -z)$ and $(-1 - x, y, -z)$ respectively.

these units is linked by an O—H···O hydrogen bond across the centre of inversion at the origin. The H atom bonded to O1 (Fig. 3, Table 2) is disordered over two sites with equal occupancy, and hence between O1 and O1^{i} [(i) $-x, -y, -z$)]

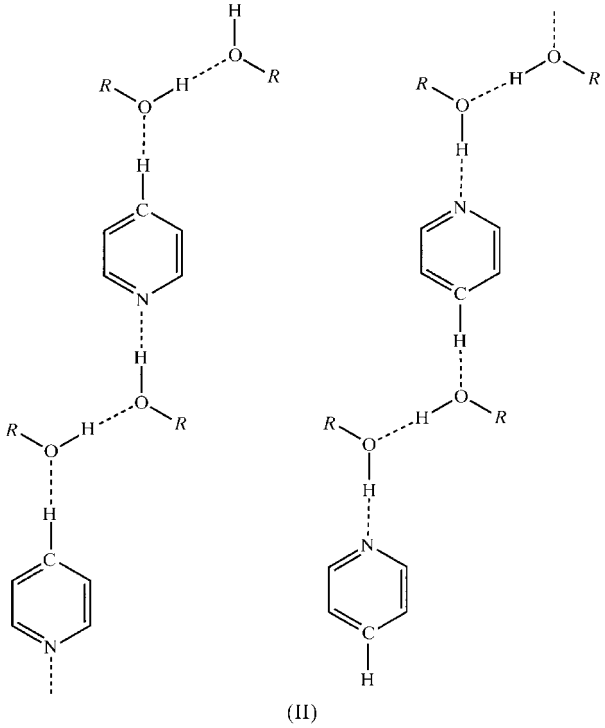

(II)

there are two possible H-atom sites, related by the centre of inversion. However, at the local level, between any such pair of O1 atoms only one of the H-atom sites can be occupied at a given instant: otherwise two hydroxylic H atoms would be required to lie within covalent bonding distance of one another. Thus, the site occupied by the hydroxylic H atom bonded to O1 effectively determines the location of the corresponding H atom bonded to O1^{i}, assuming that hydrogen bonding is always maximized at the local level, and this in turn is correlated with the orientation of the pyridine molecules [see (II), where *R* represents $C_5H_5N\cdots HO(SiPh_2O)_2SiPh_2-$].

Where a hydroxylic O1 atom acts as an acceptor in an O—H···O hydrogen bond, it necessarily carries a free, pendent H atom, and so an O—H···N hydrogen bond can be formed with the N81 of the disordered pyridine acting as an acceptor. The neighbouring symmetry-related O1^{i}, acting as the donor in the O—H···O hydrogen bond linking the two adjacent O1 sites, carries no pendent H atom, but instead acts as an acceptor in a C—H···O hydrogen bond, where the donor is the *para*-carbon C81 in the alternative orientation of the disordered pyridine. In any domain of the crystal, two such arrangements are possible [Scheme (II)]: a combination of these two static arrangements with equal probabilities yields the centrosymmetric, disordered arrangement modelled from the X-ray diffraction data. If, on the other hand, the pyridine units were able to switch easily from one orientation to the other, by rotation about the appropriate inertial axis, so interchanging N81 with the corresponding C81, then this would cause a large-scale shift of hydroxylic hydrogen bonds, probably by means of concerted rotations about the terminal Si—O bonds (Aliev *et al.*, 1995, 1998). Thus, at the local level the hard (Braga *et al.*, 1995) hydrogen bonds of O—H···N and O—H···O types link the molecular building blocks into a finite aggregate, but if the soft C—H···O hydrogen bonds are included, these finite aggregates are linked into a $C_3^3(9)$ chain running parallel to the [100] direction (Fig. 4).

3.1.3. 1,1,3,3-Tetraphenyldisiloxane-1,3-diol–hexamethylenetetramine (1/1) (3). In (3) both the diol and the hexamethylenetetramine (HMTA) units lie in general positions (Fig. 5). The diol acts as a double donor and the HMTA as a double acceptor, in the formation of two rather similar O—H···N hydrogen bonds. These hydrogen bonds serve to link the molecular components into chains running parallel to the [010] direction. Within the asymmetric unit O1 acts as a hydrogen-bond donor to N1, while O2 at (x, y, z) acts as a donor to N2 at $(x, -1 + y, z)$, thus generating by translation a

Table 3
Selected geometric parameters (Å, °).

Compound (1)			
Si1*A*—O1*A*	1.629 (2)	Si1*B*—O1*B*	1.635 (2)
Si1*A*—O2*A*	1.611 (2)	Si1*B*—O2*B*	1.618 (2)
Si2*A*—O2*A*	1.626 (2)	Si2*B*—O2*B*	1.618 (2)
Si2*A*—O2*A*	1.626 (2)	Si2*B*—O2*B*	1.618 (2)
Si2*A*—O3*A*	1.613 (2)	Si2*B*—O3*B*	1.628 (2)
Si3*A*—O3*A*	1.616 (2)	Si3*B*—O3*B*	1.635 (2)
Si3*A*—O4*A*	1.631 (2)	Si3*B*—O4*B*	1.619 (2)
N1—C1	1.321 (3)	N1—C2^{i}	1.326 (3)
C1—C2	1.372 (3)		
Si1*A*—O2*A*—Si2*A*	157.1 (1)	Si1*B*—O2*B*—Si2*B*	157.9 (1)
Si2*A*—O3*A*—Si3*A*	164.0 (1)	Si2*B*—O3*B*—Si3*B*	141.2 (1)
N1—C1—C2	121.9 (2)	N1^{i}—C2—C1	121.9 (2)
C1—N1—C2^{i}	116.3 (2)		
O1*A*—Si1*A*—O2*A*—Si2*A*	−5.7 (2)	O1*B*—Si1*B*—O2*B*—Si2*B*	−60.6 (3)
Si1*A*—O2*A*—Si2*A*—O3*A*	8.9 (2)	Si1*B*—O2*B*—Si2*B*—O3*B*	105.7 (2)
O2*A*—Si2*A*—O3*A*—Si3*A*	−129.5 (4)	O2*B*—Si2*B*—O3*B*—Si3*B*	49.6 (2)
Si2*A*—O3*A*—Si3*A*—O4*A*	78.0 (4)	Si2*B*—O3*B*—Si3*B*—O4*B*	−44.7 (2)
Compound (2)			
Si1—O1	1.625 (2)	Si2—O3	1.617 (2)
Si1—O2	1.616 (2)	Si3—O3	1.637 (2)
Si2—O2	1.612 (2)	Si3—O4	1.610 (2)
Si1—O2—Si2	163.8 (1)	Si2—O3—Si3	142.5 (1)
O1—Si1—O2—Si2	−6.6 (4)	Si1—O2—Si2—O3	−172.2 (3)
O2—Si2—O3—Si3	51.0 (2)	Si2—O3—Si3—O4	16.7 (2)
Compound (3)			
Si1—O1	1.607 (2)	Si2—O3	1.618 (2)
Si1—O3	1.618 (2)	Si2—O2	1.611 (2)
N1—C1	1.465 (3)	N3—C2	1.461 (3)
N1—C2	1.477 (3)	N3—C3	1.456 (3)
N1—C5	1.483 (3)	N3—C6	1.461 (3)
N2—C1	1.470 (3)	N4—C4	1.464 (3)
N2—C3	1.476 (3)	N4—C5	1.454 (3)
N2—C4	1.467 (3)	N4—C6	1.459 (3)
Si1—O3—Si2	162.3 (2)		
O1—Si1—O3—Si2	−3.7 (4)	Si1—O3—Si2—O2	62.2 (4)
Compound (4)			
Si1—O1	1.622 (2)	Si2—O2	1.620 (2)
Si1—O11	1.6108 (6)	Si2—O21	1.6111 (5)
Si1—O11—Si1^{ii}	180*a*	Si2—O21—Si2^{iii}	180*a*
C52—N51—C56	117.0 (2)	C62—N61—C66	117.1 (2)
Inter plane angle (N51—C56)^(N61—C66)	36.5 (1)		
Compound (5)			
Si1—O1	1.627 (2)	Si2—O2	1.621 (2)
Si1—O3	1.630 (2)	Si2—O3	1.629 (2)
N51—C52	1.317 (3)	N51—C53^{iv}	1.296 (3)
C52—C53	1.367 (4)		
Si1—O3—Si2	144.7 (1)	C52—N51—C53^{iv}	115.1 (2)
N51—C52—C53	122.6 (2)	N51^{iv}—C53—C52	122.3 (2)
O1—Si1—O3—Si2	−24.8 (2)	Si1—O3—Si2—O2	12.8 (2)
Compound (6)			
Si1—O1	1.6067 (5)	Si1—O2	1.621 (2)
Si1—O1—Si1^{v}	180†		
Compound (7)			
Si1—O1	1.6074 (5)	Si1—O2	1.623 (2)
Si1—O1—Si1^{v}	180†		

Symmetry codes: (i) $-x, 1-y, -z$; (ii) $-x, -y, -z$; (iii) $1-x, -y, 1-z$; (iv) $-1-x, -y, 1-z$; (v) $1-x, 1-y, 1-z$. † Siloxanediols lie across centres of inversion.

$C_2^2(10)$ chain (Fig. 6). The other two N atoms, N3 and N4, play no part in the hydrogen bonding; as just a double acceptor of hydrogen bonds, HMTA is adopting its most common mode of acceptor behaviour (Coupar *et al.*, 1997). Four of the $C_2^2(10)$ chains run through each unit cell, but there are no contacts between neighbouring chains shorter than the sum of van der Waals radii.

3.1.4. 1,1,3,3-Tetraphenyldisiloxane-1,3-diol–2,2′-bipyridyl (1/1) (4). In the structure of (4) there are two independent types of diol molecule: these both lie across centres of inversion, so that each contains a strictly linear Si—O—Si bridge (Fig. 7). The unique 2,2′-bipyridyl unit, by contrast, lies in a general position. Each diol acts as a double donor of hydrogen bonds, forming N—H···O bonds to two separate, but symmetry-related, bipyridyl molecules: the bipyridyl molecule acts as a double acceptor from two different diol molecules. This 1:1 combination of a double donor and a double acceptor generates a simple $C_2^2(11)$ chain motif. Within the asymmetric unit, atoms O1 and O2, which are components of the diols centred at (0, 0, 0) and ($\frac{1}{2}$, 0, $\frac{1}{2}$), respectively, act as donors to N51 and N61, respectively: the symmetry-related O1 at $(-x, -y, -z)$ in the diol centred at (0, 0, 0) acts as a donor to N51, also at $(-x, -y, -z)$, while N61 in the same bipyridyl at $(-x, -y, -z)$ accepts a hydrogen bond from O2 at $(-x, -y, -z)$, a component of the diol centred at ($-\frac{1}{2}$, 0, $-\frac{1}{2}$). Propagation of these interactions thus generates a chain (Fig. 8) running parallel to the [101] direction.

3.1.5. 1,1,3,3-Tetraphenyldisiloxane-1,3-diol–pyrazine (2/1) (5). The supramolecular structure in (5) forms a particularly elegant chain-of-rings (Bernstein *et al.*, 1995) in which cyclic centrosymmetric diol dimers alternate with pyrazine molecules, also lying

across centres of inversion. The asymmetric unit (Fig. 9) consists of just one molecule of the diol, and one half of a pyrazine molecule. Pairs of diol molecules are linked by paired O—H···O hydrogen bonds into centrosymmetric $R_2^2(12)$ dimers (Fig. 10): O2 at (x, y, z) acts as a donor to O1 at $(-x, -y, 1-z)$, leaving the two O1—H1 groups available to act as donors to the pyrazine molecules. Within the asymmetric unit O1 at (x, y, z) in the diol dimer centred at $(0, 0, \frac{1}{2})$ acts as a hydrogen-bond donor to N51 in the pyrazine centred at $(-\frac{1}{2}, 0, \frac{1}{2})$: the symmetry-related O1 at $(-x, -y, 1-z)$ in the same diol dimer in turn acts as a donor to N51, also at $(-x, -y, 1-z)$, which is part of the pyrazine centred at $(\frac{1}{2}, 0, \frac{1}{2})$. Thus, just two types of hydrogen bond, one O—H···O and one O—H···N, generate a $C_2^2(13)[R_2^2(12)]$ chain-of-rings running parallel to the [100] direction (Fig. 10).

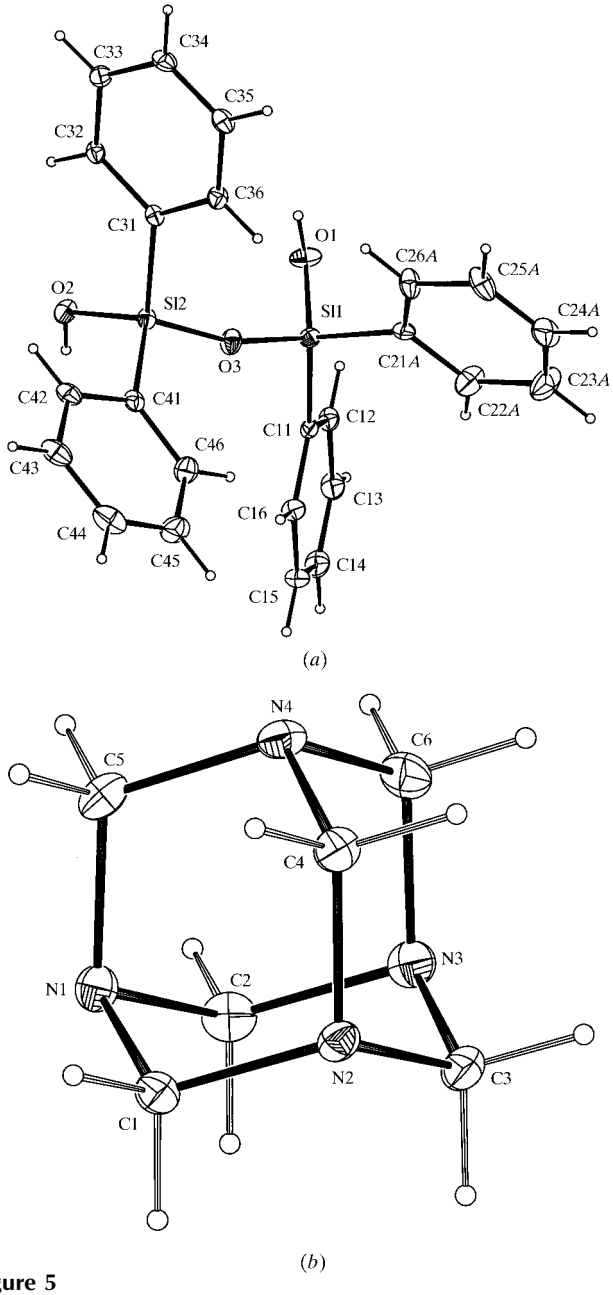

Figure 5
The molecular components of (3), showing the atom-labelling scheme: (*a*) the siloxanediol and (*b*) the HMTA. Only one orientation of the disordered phenyl ring C2*m* (*m* = 1–6) is shown. Atoms are depicted as in Fig. 1.

3.1.6. 1,1,3,3-Tetraphenyldisiloxane-1,3-diol–pyridine (1/1) (6) and 1,1,3,3-tetraphenyldisiloxane-1,3-diol–pyrimidine (1/1) (7). Although pyridine and pyrimidine might be expected to act as single and double acceptors, respectively, of hard hydrogen bonds, both these bases form adducts of 1:1 stoichiometry with 1,1,3,3-tetraphenyldisiloxane, and the crystals of the resulting compounds (6) and (7) are isomorphous. Compound (7) contains identical numbers of hydroxyl donors and nitrogen acceptors, while in (6) there is a twofold excess of donors.

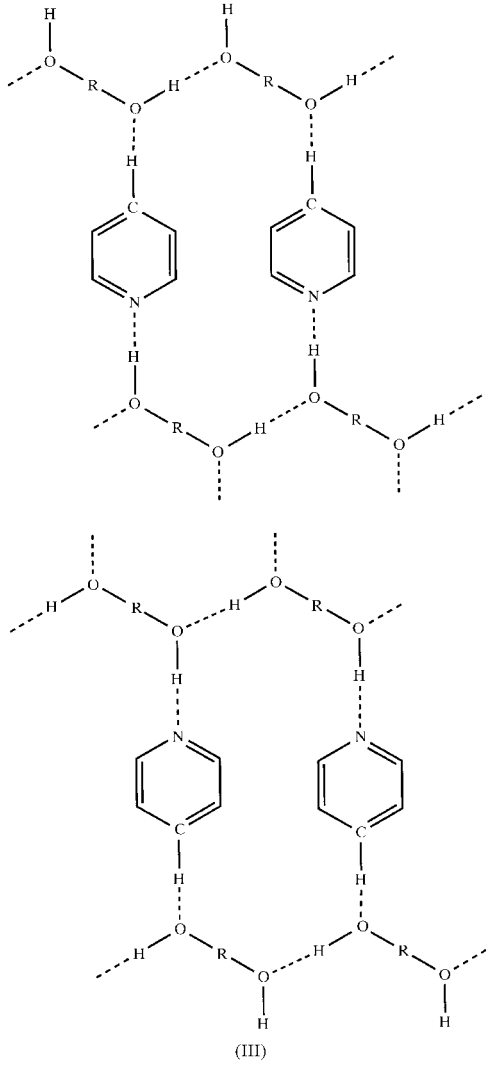

In both (6) and (7) (Figs. 11 and 12) the unit cell contains just one molecule of the diol and one of the amine: the diol components lie across centres of inversion and thus contain linear Si—O—Si units. In (6) the pyridine molecules are disordered across centres of inversion and hence appear in the average structure as pseudo-pyrazine units with half-nitrogen occupancy of two sites. The pyrimidine molecules in (7) are not only disordered across centres of inversion, but they also

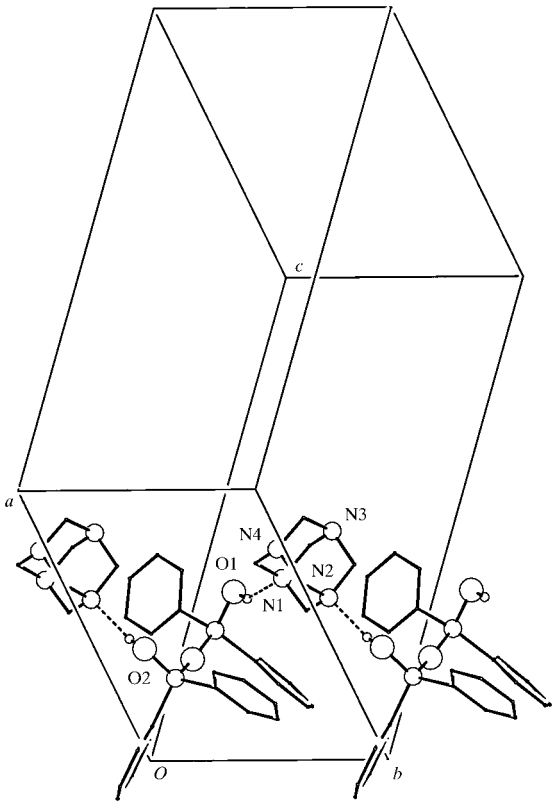

Figure 6
Part of the crystal structure of (3), showing one of the $C_2^2(10)$ chains parallel to [010]. For the sake of clarity, H atoms bonded to C are omitted.

exhibit two-site rotational disorder: the net effect of these two modes of disorder is that the site *X*31 (Fig. 12) is occupied by ($\frac{1}{2}$C+$\frac{1}{2}$N) and sites *X*32 and *X*33 are each occupied by ($\frac{3}{4}$C+$\frac{1}{4}$N).

In each of (6) and (7), the unique disiloxanediol was positioned so that it lies across the inversion centre at ($\frac{1}{2}$, $\frac{1}{2}$, $\frac{1}{2}$), and the diol molecules are linked into chains by means of O—H···O hydrogen bonds in which the H atoms are disordered. Atom O2 at (*x*, *y*, *z*) in the diol centred at ($\frac{1}{2}$, $\frac{1}{2}$, $\frac{1}{2}$) and the symmetry-related atom O2 at ($-x$, $1-y$, $1-z$), which is a component of the diol centred at ($-\frac{1}{2}$, $\frac{1}{2}$, $\frac{1}{2}$), are hydrogen bonded across the centre of inversion at (0, $\frac{1}{2}$, $\frac{1}{2}$). Between each pair of neighbouring O2 atoms, related by the inversion centres at (n, $\frac{1}{2}$, $\frac{1}{2}$) (n = zero or integer), only one of the H-atom sites can be occupied at any instant. Propagation of these interactions generates a $C(6)$ chain running parallel to the [100] direction (Fig. 13).

The role of the disordered amine units, whether pyridine in (6) or pyrimidine in (7), in linking these one-dimensional aggregates, the $C(6)$ chains, into a two-dimensional network is entirely analogous to the role of pyridine in (2) in linking finite, zero-dimensional aggregates into a continuous one-dimensional system, in that case a $C_3^3(9)$ chain. In an entirely similar manner to the action of pyridine in (2), the amine units in (6) and (7) give rise to $C_3^3(9)$ chains running parallel to the [001] direction: the combination of the [100] and [001] chains generates a continuous two-dimensional net parallel to (010) and built from a single type of $R_6^6(26)$ ring [Fig. 13 and Scheme (III), where *R* represents —$SiPh_2OSiPh_2$—].

3.2. Hydrogen-bond dimensions

The hydrogen bonds of O—H···O and O—H···N types are all reasonably short for such bonds involving only neutral donors and acceptors. The O···O distances (Table 2) range between 2.673 (2) Å in (1) and 2.809 (2) Å in (2), while the O—H···O angles have an average value of 164°, close to the most frequently observed value, 160° (Jeffrey & Saenger, 1991). The O···N distances in O—H···N hydrogen bonds involving fully ordered amine acceptors, *i.e.* those in (1) and (3)–(5), range from 2.706 (2) Å in (1) to 2.869 (2) Å in (2); the mean value of the O—H···N angle in the fully ordered cases is 157°, again close to 160° (Jeffrey & Saenger, 1991).

In (2), (6) and (7) the $D\cdots A$ distances involving the disordered pyridine, in (2) and (6), or pyrimidine in (7), represent a compromise between the ideal, minimum-energy distance for O—H···N and C—H···O hydrogen bonds. Hence, the O···N distances in these examples are rather long for their type and the C···O distances are correspondingly short.

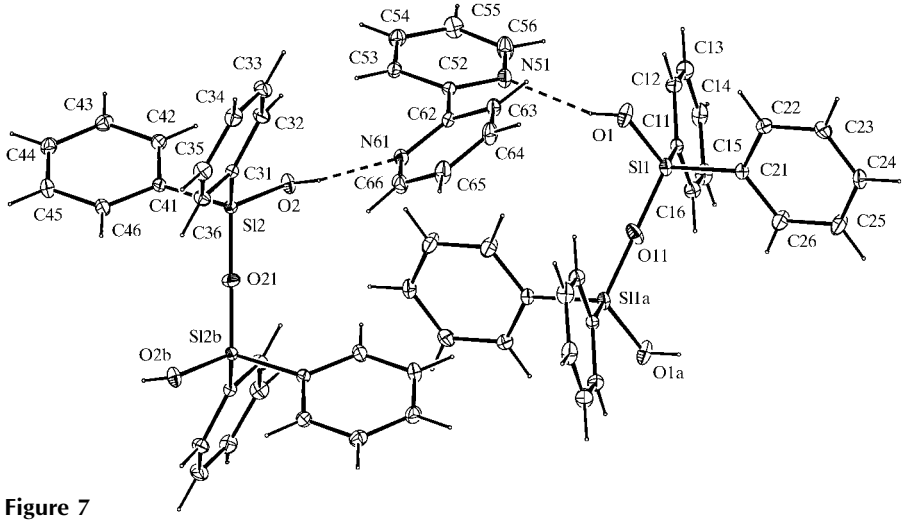

Figure 7
The molecular components of (4), showing the atom-labelling scheme. Atoms are depicted as in Fig. 1.

3.3. Molecular geometries

3.3.1. Disiloxane components. The most striking feature of the disiloxanediol component in (3)–(7) is the variation in the geometry of the Si—O—Si fragments. The disiloxanediol components in (4), (6) and (7) contain strictly linear Si—O—Si bridges, since these molecules lie across centres of

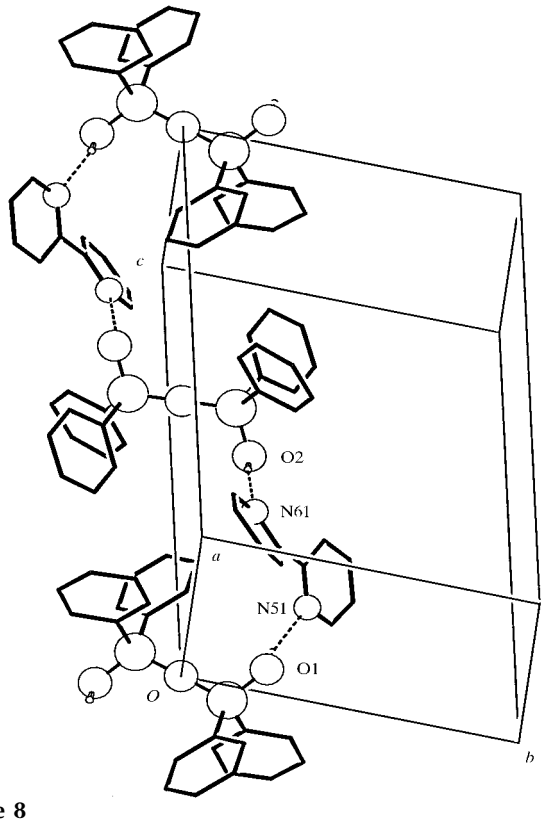

Figure 8
Part of the crystal structure of (4), showing one of the $C_2^2(11)$ chains parallel to [101]. For the sake of clarity, H atoms bonded to C are omitted.

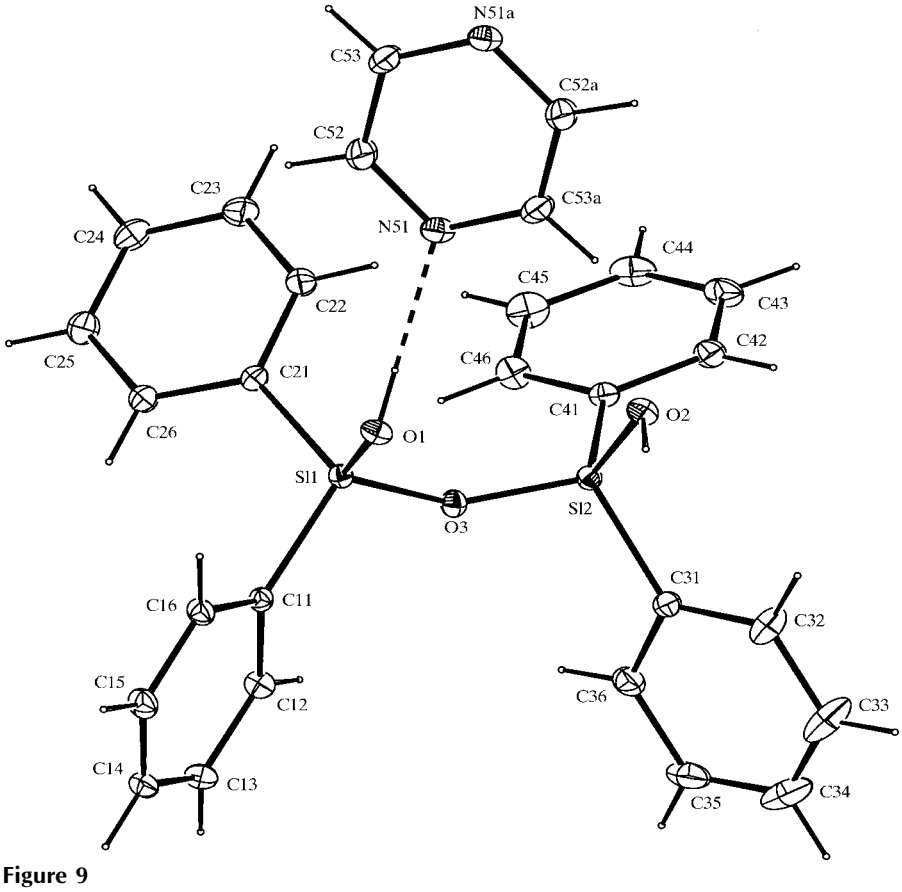

Figure 9
The asymmetric unit of (5), showing the atom-labelling scheme. Atoms are depicted as in Fig. 1.

inversion (Figs. 7, 11 and 12); in (3) and (5), on the other hand, the Si—O—Si angles are 162.3 (2) and 144.7 (1)°, respectively (Table 3). In the pure diol (Hossain & Hursthouse, 1988), where the asymmetric unit contains three molecules, the Si—O—Si angles range from 147.8 (3) to 162.5 (3)°, while in the 3:2 adduct formed by the diol with pyridazine (Ruud *et al.*, 1991) the structure contains both linear and bent (144.5°) Si—O—Si diol units.

These observations are consistent with the occurrence of an extremely low bending force constant for linear Si—O—Si, so that the geometry of this fragment is readily perturbed by intermolecular forces. If the deviation from linearity of the Si—O—Si fragment is denoted by θ, the bending potential function $V(\theta)$ can be represented by an harmonic-quartic function (Glidewell *et al.*, 1972)

$$V(\theta) = A\theta^4 - B\theta^2. \quad (1)$$

This function exhibits a barrier of height $(B^2/4A)$ at $\theta = 0$ separating two minima at $\theta = \pm(B/2A)^{1/2}$. When B is small relative to A, the $v = 0$ vibrational level lies above the barrier and this allows the system to bend in the range $\theta = \pm(B/A)$ with essentially no energy cost. The trisiloxanediol components in (1) and (2) also exhibit a range of Si—O—Si angles spanning over 20°, again consistent with a very low force constant for the bending of the Si—O—Si unit.

In (1)–(3) and (5), where the Si—O—Si units are all non-linear, there is no systematic difference between Si—O distances of Si—O—(Si) and Si—O—(H) types. However, in (4), (6) and (7), where the diol units lie across centres of inversion with consequent linearity of the Si—O—Si bridges, the Si—O distances to the bridging O are systematically and significantly shorter than the terminal Si—O distances. Similarly short Si—O distances, less than 1.62 Å, have been reported previously in a number of molecular systems containing linear Si—O—Si bridges, including $(Ph_3Si)_2O$, 1.616 (1) Å (Glidewell & Liles, 1978), $[(PhCH_2)_3Si]_2O$, 1.613 (4) Å (Glidewell & Liles, 1981), $[^tBu(OH)_2Si]_2O$, 1.600 (1) Å (Lickiss *et al.*, 1991), the pyridazine adduct of 1,1,3,3-tetraphenyldisiloxane-1,3-diol, 1.601 (4) Å (Ruud *et al.*, 1991), and $[Ph_2(MeNHNH)Si]_2O$, 1.6131 (13) Å (He *et al.*, 1994). The Si—C distances are all typical of their type (Allen *et al.*, 1987).

The conformations of the diol components show marked deviations from full staggering about the skeletal Si—O bonds (Table 3), while this is a necessary consequence

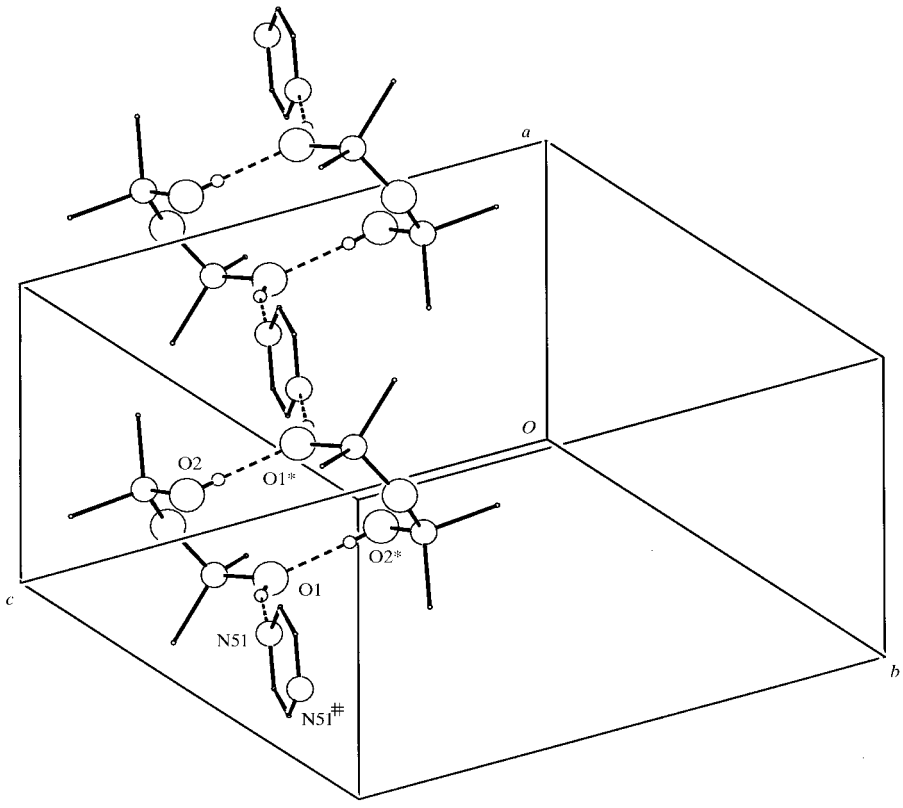

Figure 10
Part of the crystal structure of (5), showing a $C_2^2(13)$ [$R_2^2(12)$] chain-of-rings parallel to [100]. For the sake of clarity, only the C*n*1 (n = 1–4) atoms of the phenyl rings are shown; the H atoms of the pyrazine component are also omitted. The atoms labelled with a star (*) or hash (#) are at symmetry positions $(-x, -y, 1-z)$ and $(-1-x, y, 1-z)$, respectively.

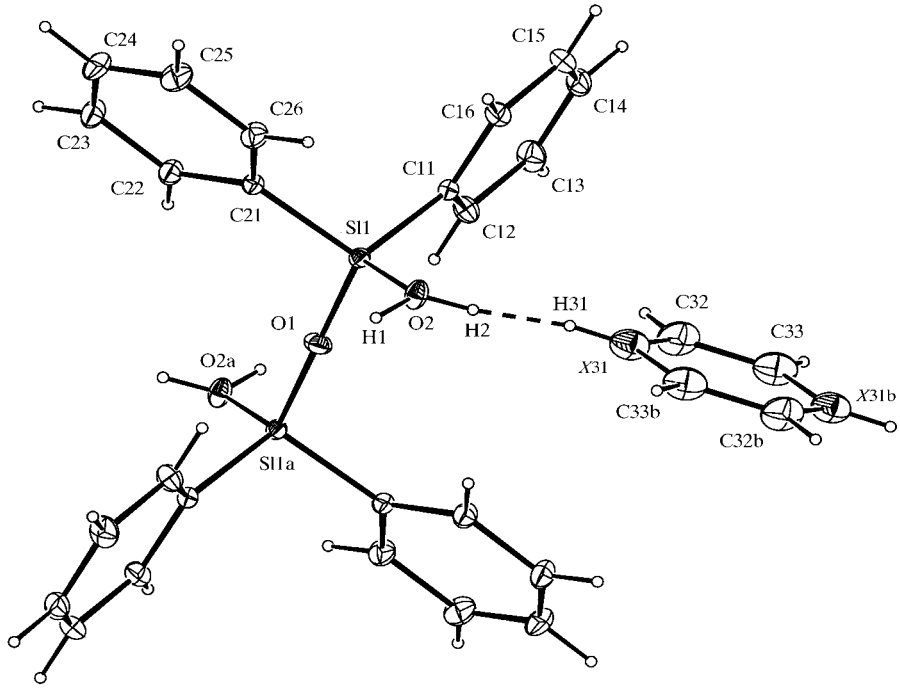

Figure 11
The molecular components of (6), showing the atom-labelling scheme. Atoms are depicted as in Fig. 1. Atoms marked 'a' and 'b' are at symmetry positions $(1-x, 1-y, 1-z)$ and $(-x, 1-y, 2-z)$, respectively. The site *X*31 in the disordered pyridine is occupied by ($\frac{1}{2}$C + $\frac{1}{2}$N): the occupancies of the H1, H2 and H31 sites are all $\frac{1}{2}$ (see text).

of the cyclic dimer formation in (1) and (5), it is perhaps unexpected in (2) and (3). The rotational barriers about the Si—O bonds may be lower than those normally encountered for single bonds in organic molecules because of the larger radius of Si: in any event, as with the Si—O—Si angles, the effect of the intermolecular forces, specifically the hydrogen bonds, is sufficient to perturb the diol components from their energy minima.

3.3.2. Amine components. In (3), there is a significant difference between those C—N bond lengths in the HMTA component which involve the hydrogen-bond acceptor and the remainder (Table 3): those bonds involving N1 and N2 (Table 2) span the range 1.465 (3)–1.483 (3) Å, with mean 1.473 Å, whereas those involving N3 and N4 span the range 1.454 (3)–1.464 (3) Å, with mean 1.459 Å. This is entirely consistent with the pattern of behaviour previously observed in hydrogen-bonded adducts of HMTA (Coupar *et al.*, 1997), although the difference in mean C—N distance is much less than those observed in protonated HMTA (Mak *et al.*, 1983; Chou *et al.*, 1987; Tebbe & Nagel, 1995).

In (1), (4) and (5), where the heteroaromatic amines are fully ordered, the C—N—C bond angles are all significantly less than 120°, reflecting the greater electronegativity of N and mimicking the effect of an electronegative substituent at this position (Domenicano & Murray-Rust, 1979).

4. Concluding comments

In the supramolecular structures of (1)–(7), the formation of O—H···N hydrogen bonds between the siloxanediols and the amines is always accompanied by the formation of O—H···O hydrogen bonds: these are usually intermolecular. The diversity both of the stoichiometries of the adducts and of the dimen-

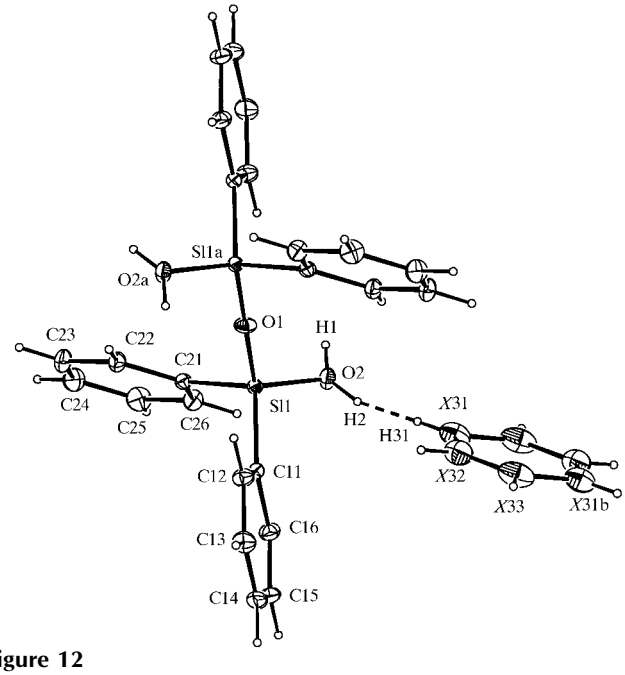

Figure 12
The molecular components of (7), showing the atom-labelling scheme. Atoms are depicted as in Fig. 11. The site *X*31 in the disordered pyrimidine is occupied by ($\frac{1}{2}$C + $\frac{1}{2}$N): the sites *X*32 and *X*33 are occupied by ($\frac{3}{4}$C + $\frac{1}{4}$N). The occupancy of the H1, H2 and H31 sites is $\frac{1}{2}$; the occupancy of the H32 and H33 sites is $\frac{3}{4}$ (see text).

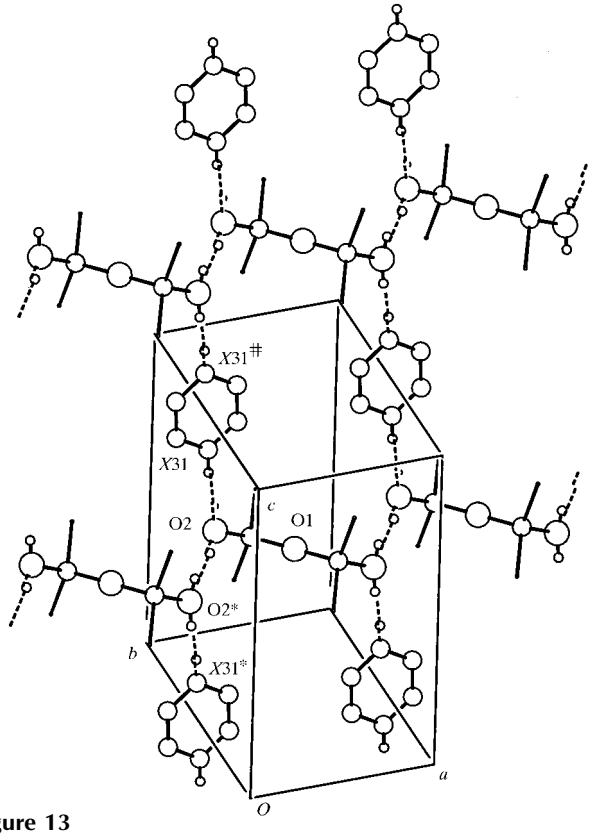

Figure 13
Part of the crystal structure of (6) and (7), showing one of the $R_6^6(26)$ rings forming the net parallel to (010). For the sake of clarity, only the C11 and C21 atoms of the phenyl rings are shown; the H atoms of the amine component are also omitted. Atoms marked with a star (*) or hash (#) are at symmetry positions $(-x, 1-y, 1-z)$ and $(-x, 1-y, 2-z)$, respectively.

sionality of their structures indicate that structural prediction in this series remains difficult. Similarly hard to predict is the skeletal geometry of the siloxanediol component, rendered difficult by the ease with which the Si—O—Si bridge angle is perturbed by the intermolecular forces.

References

Aliev, A. E., Harris, K. D. M., Shannon, I. J., Glidewell, C., Zakaria, C. M. & Schofield, P. A. (1995). *J. Phys. Chem.* **99**, 12008–12015.

Aliev, A. E., MacLean, E. J., Harris, K. D. M., Kariuki, B. M. & Glidewell, C. (1998). *J. Phys. Chem.* **102**, 2165–2175.

Allen, F. H., Kennard, O., Watson, D. G., Brammer, L., Orpen, A. G. & Taylor, R. (1987). *J. Chem. Soc. Perkin Trans. 2*, pp. S1–S19.

Behbehani, H., Brisdon, B. J., Mahon, M. F. & Molloy, K. C. (1993). *J. Organomet. Chem.* **463**, 41–45.

Bernstein, J., Davis, R. E., Shimoni, L. & Chang, N.-L. (1995). *Angew. Chem. Int. Ed. Engl.* **34**, 1555–1573.

Braga, D., Grepioni, F., Biradha, K., Pedireddi, V. R. &. Desiraju, G. R. (1995). *J. Am. Chem. Soc.* **117**, 3156–3166.

Chou, M., Lessinger, L. & Chiang, M. (1987). *Acta Cryst.* C**43**, 322–324.

Coupar, P. I., Glidewell, C. & Ferguson, G. (1997). *Acta Cryst.* B**53**, 521–533.

Domenicano, A. & Murray-Rust, P. (1979). *Tetrahedron Lett.* pp. 2283–2286.

Ferguson, G., Gallagher, J. F., Glidewell, C. & Zakaria, C. M. (1993*a*). *Acta Cryst.* C**49**, 967–971.

Ferguson, G., Gallagher, J. F., Glidewell, C. & Zakaria, C. M. (1993*b*). *J. Chem. Soc. Dalton Trans.* pp. 3499–3506.

Ferguson, G., Glidewell, C., Lewis, A. & Zakaria, C. M. (1995). *J. Organomet. Chem.* **492**, 229–234.

Glidewell, C., Ferguson, G., Lough, A. J. & Zakaria, C. M. (1994). *J. Chem. Soc. Dalton Trans.* pp. 1971–1982.

Glidewell, C. & Liles, D. C. (1978). *Acta Cryst.* B**34**, 124–128.

Glidewell, C. & Liles, D. C. (1981). *J. Organomet. Chem.* **212**, 291–300.

Glidewell, C., Robiette, A. G. & Sheldrick, G. M. (1972). *Chem. Phys. Lett.* **16**, 526–529.

Harris, G. I. (1963). *J. Chem. Soc.* pp. 5978–5982.

He, J., Harrod, J. F. & Hynes, R. (1994). *Organometallics*, **13**, 2496–2499.

Hossain, M. A. & Hursthouse, M. B. (1988). *J. Crystallogr. Spectrosc. Res.* **18**, 227–234.

Jeffrey, G. A. & Saenger, W. (1991). *Hydrogen Bonding in Biological Structures.* Berlin: Springer-Verlag.

Lickiss, P. D. (1995). *Adv. Inorg. Chem.* **42**, 147–262.

Lickiss, P. D., Litster, S. A., Redhouse, A. D. & Wisener, C. J. (1991). *J. Chem. Soc. Chem. Commun.* pp. 173–174.

Lickiss, P. D., Redhouse, A. D., Thompson, R. J., Stanczyk, W. A. & Rózga, K. (1993). *J. Organomet. Chem.* **453**, 13–16.

Mak, T. C. W., Li, W.-K. & Yip, W.-H. (1983). *Acta Cryst.* C**39**, 134–136.

Prescott, P. I. & Selin, T. G. (1965). US Patent 3,222,369; *Chem. Abs.* 64, 5136*c* (1966).

Ruud, K. A., Sepeda, J. S., Tibbals, F. A. & Hrncir, D. C. (1991). *J. Chem. Soc. Chem. Commun.* pp. 629–630.

Selin, T. G. (1977). US Patent 4,003,917; *Chem. Abs.* 86, 155790g (1977).

Sheldrick, G. M. (1997). *SHELXL*97. University of Göttingen, Germany.

Tebbe, K.-F. & Nagel, K. (1995). *Z. Anorg. Allg. Chem.* **621**, 225–228.